Phonon-mediated intervalley relaxation of positive trions in monolayer WSe_{2}

Keisuke Shinokita, Xiaofan Wang, Yuhei Miyauchi, Kenji Watanabe, Takashi Taniguchi, Satoru Konabe, and Kazunari Matsuda

Phys. Rev. B **100**, 161304 — Published 21 October 2019

DOI: 10.1103/PhysRevB.100.161304

Phonon-mediated Intervalley Relaxation of Positive Trions in Monolayer WSe_2

Keisuke Shinokita[1,†], Xiaofan Wang[1], Yuhei Miyauchi[1], Kenji Watanabe[2], Takashi Taniguchi[2], Satoru Konabe[3], and Kazunari Matsuda[1,*]

[1]*Institute of Advanced Energy, Kyoto University, Uji, Kyoto 611-0011, Japan*

[2]*National Institute for Materials Science, 1-1 Namiki, Tsukuba, Ibaraki 305-0044, Japan*

[3]*Department of Chemical Science and Technology, Hosei University, Koganei, Tokyo 184-8584, Japan*

Abstract

The valley relaxation mechanism of the bright state of positively charged excitons (bright positive trions) in monolayer (1L-) WSe_2 is studied through polarization- and time-resolved photoluminescence and transient reflection measurements. A long valley relaxation time, exceeding 100 ps, is observed for positive trions at low temperature, which is notably prolonged when compared with the characteristic excitonic valley relaxation time of 10 ps. With increasing temperature, the relaxation time decreases to a few ps. This finding implies that phonon-mediated intervalley scattering is important for the relaxation process of the valley-polarized bright state of positive trions.

†shinokita.keisuke.4r@kyoto-u.ac.jp

*matsuda@iae.kyoto-u.ac.jp

Keywords: Valley polarization, transition metal dichalcogenides, charged exciton

The monolayers of transition metal dichalcogenides (TMDs) composed of MX_2 (M = Mo, W; X = S, Se, Te) have recently attracted substantial attention for fundamental and applied physics because of their novel optical and electrical properties [1,2]. The novel physical properties originate from reduced dimensionality in monolayer TMDs and are dominated by many-body excitonic effects due to the strongly Coulomb-bounded electrons and holes, including neutral excitons and charged excitons (trions) [3,4,13,5–12]. In addition, a direct bandgap at K and $-K$ valleys in the corners of the two-dimensional hexagonal Brillouin zone gives rise to valley degrees of freedom [14–22]. The large spin-orbit interaction and lack of spatial inversion symmetry in monolayer TMDs couple the valley and spin degrees of freedom (spin-valley locking), which enables the selective excitation and detection of excitons and trions at the K and $-K$ valleys by shining circularly polarized light (valley-polarized states or valley polarization of excitons and trions).

Of particular interest is the relaxation mechanism of valley polarization. Thus far, substantial efforts in experimental and theoretical studies have been successfully devoted to elucidate the valley relaxation mechanism of neutral excitons [16,23–29]. However, the relaxation mechanism of trions is not yet understood, even though trions are of fundamental interest and practical importance for excitonic valley-polarized phenomena in the electrical detection and manipulation of trions through the valley Hall effect [17,21,38–40,30–37]. Previous studies using time-resolved photoluminescence (PL), pump-probe, and Kerr rotation spectroscopy have reported stable valley polarization of trions [17,36,38,40,41], suggesting that the valley relaxation mechanism of trions differs from that of neutral excitons in which momentum-dependent long-range

electron–hole exchange interactions play a crucial role. Understanding the valley relaxation mechanism of trions requires further studies, including an investigation of temperature-dependent valley relaxation dynamics, which would provide important information regarding trion–phonon interactions in the valley physics of atomically thin TMDs.

In this work, we studied the valley relaxation mechanism of positive trions in monolayer (1L-) WSe_2 based on the polarization- and time-resolved PL and transient reflection spectroscopy. We evaluated the temperature-sensitive valley polarization and relaxation time of positive trions. A long valley relaxation time (>100 ps) was observed for positive trions at 10 K, showing considerably stable valley polarization when compared with excitonic valley polarization. As the temperature increases to above 100 K, the valley relaxation occurs more rapidly on a timescale of a few ps. This finding implies that phonon-mediated intervalley scattering is important for the valley relaxation of bright positive trions.

We studied the mechanically exfoliated 1L-WSe_2 on a Si substrate with a 270-nm thick insulating SiO_2 layer. A field-effect transistor structure with Pt electrodes was fabricated by a dry-transfer process [41], and capped with hexagonal boron nitride (hBN). The application of a back-gate voltage V_g enables to inject carriers to the 1L-WSe_2. The doped hole density was 2×10^{12} cm^{-2} under a gate voltage V_g of −40 V [29,42].

To measure the valley relaxation dynamics, we performed polarization- and time-resolved PL and transient reflection measurements. Polarization-resolved time-integrated and time-resolved PL spectroscopy techniques were applied, with a continuous wave He–Ne laser (photon energy of 1.959 eV, power of 10 μW) and a pulsed supercontinuum laser (photon energy of 1.922 eV, power of 45 μW, pulse duration of ~20 ps, repetition rate of 40 MHz), respectively. In the pump-probe measurement in reflection geometry, a ~200-fs pump pulse (central wavelength of 680 nm, repetition rate of 1 MHz, pump power of 1 μW) was focused on the 1L-WSe_2 sample with a spot diameter of 2 μm, resulting in an excitation density of $N \approx 10^{12}$ /cm^2 electron–hole pairs, which is in the linear regime [43]. A white-light probe pulse generated using a yttrium-aluminum-garnet (YAG) crystal was detected by a photodiode after the pulse passed through a monochromator [41].

A schematic of the *K*-valley configurations of the spin-allowed bright states of the positively charged excitons (positive trions) under hole-doped conditions are shown in Figure 1(a). The band structure of 1L-WSe_2 exhibits valley-dependent spin splitting of the conduction and valence bands because of the strong spin-orbit couple [44]. The optically allowed bright trions couple with light in an efficient manner, resulting in dominant radiative recombination as a PL process.

Figure 1(b) shows the helicity-resolved PL spectra for a gate voltage of −40 V at various temperatures under σ_+ circularly polarized laser (selective *K*-valley excitation).

Two prominent peaks were observed, particularly at a low temperature. The emission peaks on the higher (>1.7 eV) and lower (<1.7 eV) energy sides correspond to the recombination process of bright positive trions (T^+) and localized excitons in defect states (L), respectively [17,32,45]. At 10 K, the σ_+ component of the PL spectra of the trions (red curves) is more intense than the σ_- component (black curves). The more population of bright trions in the pumped *K* valley reflects valley polarization or the valley-polarized state of positive trions in 1L-WSe_2. With increasing temperature, the σ_+ and σ_- components exhibit similar PL intensities, indicating that the valley polarization is lost at high temperatures.

Figure 1(c) shows the valley polarization of bright positive trions ρ as a function of temperature for a gate voltage of −40 V (red circles). The valley polarization was estimated as $\rho = (I_{\sigma_+} - I_{\sigma_-})/(I_{\sigma_+} + I_{\sigma_-})$, where $I_{\sigma+}$ and $I_{\sigma-}$ are the σ_+ and σ_- components of the trion PL intensities, respectively [16,17,19]. The valley polarization at low temperature was ~0.4 and decreased to 0 as the temperature increased above 100 K. This result shows that the valley-polarized bright state of positive trions is sensitive to temperature.

The valley polarization of bright trions ρ in the PL measurement is phenomenologically provided by [14,16,27,31,32,46]

$$\rho = \frac{\rho_0}{1 + \frac{\langle \tau_T \rangle}{\tau_v}}, \#(1)$$

where ρ_0 is the initially created valley polarization by the circularly polarized light, $\langle\tau_T\rangle$ is the mean bright trion lifetime, and τ_v is the scattering time of bright trions between the K and $-K$ valleys. Based on Eq. (1), the initial valley polarization ρ_0 and mean trion lifetime $\langle\tau_T\rangle$ give an estimation of the valley relaxation time τ_v.

To evaluate the mean trion lifetime, we performed time-resolved PL measurements. Figure 2(a) shows the time-resolved PL decay of positive trions at −40 V for various temperatures (red circles) and the instrument response function (IRF) of the experimental setup (black curves). As the temperature increases, the decay occurs more slowly. The PL decays were fitted using a double-exponential function as $I = A_1 \exp(-t/\tau_1) + A_2 \exp(-t/\tau_2)$ convoluted with the IRF, where A_1 and A_2 denote the amplitudes and τ_1 and τ_2 denote the time constants. The experimental transients fit well, as shown by the green curves. The temperature dependence of the mean trion lifetime defined as $\langle\tau_T\rangle = (A_1\tau_1 + A_2\tau_2)/(A_1 + A_2)$ is shown in Fig. 2(c) (red circles). The mean trion lifetime increased with increasing temperature.

To further understand the temperature dependence of the PL decay, we performed two-color pump-probe spectroscopy to study the nonradiative decay of the dark state. A pump pulse of 1.824 eV excites electrons from the first valence band (VB1) to the second conduction band (CB2) [Inset of Fig. 2(b)]. The resulting reflectance change was measured by visible probe pulse monitoring to the B transition between the second valence band (VB2) and the first conduction band (CB1) [47]. The probe photon energy was tuned to the B transition energy at each temperature. The B transition provides

information regarding the spin-forbidden dark trion state since the final state of the B transition (CB1) is occupied by electrons that form dark trions, and the formation and change of the dark trion wavefunction affect the transition [37,41,48]. Figure 2(b) shows the pump-probe traces at different temperatures, demonstrating that the decay occurs more rapidly as the temperature increases. Fitting the traces using a monoexponential function well reproduces the experimentally obtained pump-probe signals (green curves). The pump-probe decay times of the B transition are also shown as a function of temperature in Fig. 2(c) (blue open triangles). The pump-probe decay of ~200 ps at low temperature is similar with the reported value of dark trion lifetime [49]. The pump-probe decay occurs more rapidly as the temperature increases, and the decay of dark excitons is accelerated as the temperature increases.

The increased mean lifetime of bright trions and the faster decay of dark trions at higher temperatures suggest that phonon scattering mixes the spin-allowed bright and spin-forbidden dark states of positive trions, similar to neutral excitons [50]. The relaxation process from the bright to dark state has been reported to depend on the momentum of the bright trions through phonon scattering [41,47]; thus, for simplicity, we classified bright trions with small ($k \sim 0$) and large ($k \neq 0$) momentum under photoexcitation with a finite laser energy bandwidth. The temperature dependence of the trion dynamics was modeled with the following rate equation based on the bright, dark, and ground states, as shown in Fig. 2(d):

$$\frac{dN_{\mathrm{B},k\neq0}}{dt} = \alpha G - \gamma_{k\neq0} N_{\mathrm{B},k\neq0},$$
$$\frac{dN_{\mathrm{B},k\sim0}}{dt} = (1-\alpha)G - [\Gamma_{\mathrm{b}} + \gamma_{k\sim0}(n+1)]N_{\mathrm{B},k\sim0} + \gamma_{k\sim0} n N_{\mathrm{D}},$$
$$\frac{dN_{\mathrm{D}}}{dt} = \gamma_{k\sim0}(n+1)N_{\mathrm{B},k\sim0} + \gamma_{k\neq0} N_{\mathrm{B},k\neq0} - [\Gamma_{\mathrm{d}} + \gamma n]N_{\mathrm{D}}, \#(2)$$

where G is the optical generation rate of the photocarriers, α is the ratio of bright trions with finite momentum ($k \neq 0$) to the total number of photoexcited bright trions, and $N_{\mathrm{B},k\sim0}$, $N_{\mathrm{B},k\neq0}$, and N_{D} are the populations of bright trions with small and large momentum and dark trions, respectively. Γ_{b} (Γ_{d}) represents the radiative (nonradiative) decay of bright (dark) trions, $\gamma_{k\sim0}$ and $\gamma_{k\neq0}$ are the phonon-scattering rates of bright trions with small and large momentum to the dark state, respectively, and $n = 1/(\exp(\Delta_{\mathrm{BD}}/k_{\mathrm{B}}T)-1)$ is the phonon occupation number, in which Δ_{BD} is the energy difference between the bright and dark state, k_{B} is Boltzmann's constant, and T is the temperature. The slow radiative decay of the dark trions is not taken into the consideration because the dark trions mainly decay nonradiatively [51].

The time-dependent populations of bright and dark trions are calculated using the parameters of $\alpha = 0.95$, $\gamma_{k\sim0} = (16\ \mathrm{ps})^{-1}$, $\gamma_{k\neq0} = (0.4\ \mathrm{ps})^{-1}$, and $\Delta_{\mathrm{BD}} = 20$ meV [41,48,50]. The temperature-dependent PL decay and pump-probe decay at the B transition monitoring the populations of bright and dark trions, respectively, are well reproduced, as shown in Fig. 2(c) (solid curves). The agreement indicates that the PL and pump-probe decay times are related to the phonon-assisted population transfer of positive trions between bright and dark states [52–54]. The photogenerated bright trions with large momentum ($k \neq 0$) efficiently relax to lower-lying dark states on a sub-picosecond timescale through phonon scattering, while the bright trions with small

momentum (k~0) are more stable against relaxation to the dark state. At low temperatures, the dark trions cannot populate the bright state due to the limited number of phonons. As the temperature increases, population transfer from the dark state to the bright state occurs due to phonon scattering, which gives rise to another relaxation channel and a faster population decay of dark trions.

Based on the above trion dynamics, we focus on the relaxation time of the valley-polarized bright positive trions because the dark trions are generated as valley nonpolarized state in the experimental geometry [41]. From Eq. (1) and the bright trion lifetime shown in Fig. 2(c), the valley relaxation time τ_v can be estimated. Here we set the temperature-independent value of ρ_0 as ~0.4 based on polarization-resolved PL decay measurements regardless of the excitation photon energy because the valley polarization is insensitive to the excitation photon energy unless the photon energy is resonant with 2s excited bright exciton state [31,41,55]. Figure 3 shows the estimated valley relaxation time as a function of temperature. The similarity between ρ and ρ_0 at low temperatures (<30 K) indicates a very long valley relaxation time of more than 100 ps at low temperatures. As the temperature increases, the valley relaxation time decreases, approaching a few ps above 100 K. This temperature dependence demonstrates that the valley relaxation processes of bright trions are very sensitive to temperature.

Based on these clarified valley dynamics, we further investigated the relaxation mechanism of the valley-polarized bright state of positive trions. The significantly long

trion valley relaxation time (>100 ps) at 10 K when compared to that of the excitons (~10 ps) [31] suggests a different mechanism for the valley scattering process of the neutral and charged excitons. The relaxation process of the valley-polarized state of neutral excitons has been reported to mainly suffer momentum-dependent long-range electron–hole exchange interactions [16,23–28], whereas the exchange interaction in the positive trions is expected to be suppressed by additional holes because the reduced trion oscillator strength under hole doping due to Pauli blocking [56] should weaken the off-diagonal coupling among different valley configurations due to the exchange interactions [57,58]. The screening effect due to doped holes would also weaken the exchange interaction [31], which would prolong the valley relaxation. The qualitative agreement with the stable valley polarization of positive trions in the experiment indicates that the exchange interaction is expected to play a minor role in the relaxation process of the valley-polarized bright state of positive trions.

The temperature-sensitive valley relaxation process suggests that the phonon-mediated intervalley scattering of positive bright trions plays a dominant role at finite temperatures [48,59]. In the phonon-mediated scattering process, the valley relaxation time τ_v is described as

$$\tau_v^{-1} = \Gamma_0 + \frac{\Gamma_1}{\exp\left(\frac{E_{\text{phonon}}}{k_B T}\right) - 1}, \#(3)$$

where Γ_0 is the zero-temperature intervalley scattering rate, Γ_1 is the phonon-mediated intervalley scattering rate, and E_{phonon} is the involved phonon energy. The out-of-plane A_{1g} and in-plane E^1_{2g} phonons near the K valley at 210 cm^{-1} are candidates for mediating such a scattering process between the K and -K valleys because their energy

(~25.2 meV) is close to that of the conduction band splitting in the *K* valley (~40 meV) [44,60–63]. Although intervalley scattering requires a spin-flip process, a Fermi−Dirac distribution of large-momentum trions at high temperatures would lead to an ultrafast spin-flip phonon-mediated process within picoseconds [41,48]. By assuming that the phonons near the *K* valley cause valley relaxation, the valley relaxation time can be calculated using the parameters of E_{phonon}~23 meV, Γ_0 = (100-1500 ps)$^{-1}$, and Γ_1 = (0.4 ps)$^{-1}$, as shown in Fig. 3 (green filled curve). The phonon-mediated valley scattering process well reproduces the experimentally observed valley relaxation time. The calculated valley polarization, as shown in Fig. 1 (c) (green), also explains the temperature dependence, which strongly implies that phonon-mediated valley scattering is the dominant valley relaxation mechanism of bright positive trions in 1L-WSe_2 [Inset of Fig. 3].

In conclusion, we have investigated the valley relaxation dynamics of positive trions in 1L-WSe_2. We evaluate the slow valley relaxation for bright trions (>100 ps), which is significantly slower than the characteristic excitonic valley relaxation (10 ps). The results suggest that the electron–hole exchange interaction is reduced in three-body trion systems due to the presence of additional holes. In addition, the valley relaxation time is sensitive to temperature and becomes very short at temperatures above 100 K. These findings suggest that phonon-mediated intervalley scattering plays an important role in the relaxation process of the valley-polarized bright state of the positive trions.

This work was supported by JSPS KAKENHI (Grant No. JP16H00911, JP15K13337,

JP15H05408, JP15K13500, JP16H00910, JP16H06331, JP17H06786, JP17K19055, and 19K14633), by JST CREST (Grant No. JPMJCR16F3 and JPMJCR18I5), by the Keihanshin Consortium for Fostering the Next Generation of Global Leaders in Research (K-CONNEX) established by the Human Resource Development Program for Science and Technology, MEXT, by ATI Research Grants 2017, and by the Asahi Glass Foundation.

Figure captions

Figure 1. (a) Valley configurations of the bright state of a positively charged exciton (bright positive trion) in the *K* valley in 1L-WSe_2. The red and green lines denote the spin-up and spin-down conduction/valence bands, respectively. The -*K* bright trion state represents the time reversal of the schematics. (b) Helicity-resolved PL spectra for a gate voltage of −40 V under σ_+ CW excitation at different temperatures. The red (black) curves show the PL spectra for the σ_+ (σ_-) component. (c) Temperature dependence of the valley polarization of bright positive trions for a gate voltage of −40 V (red circles). The green curve is the valley polarization calculated from Eq. (1) and (3).

Figure 2. (a) PL decay traces of positive trions under pulsed excitation at various temperatures for a gate voltage of −40 V (red circles), and fitting profiles obtained from the convolution of the double-exponential decay with the IRF (green curves). The black curve is the IRF. (b) Pump-probe traces near the B transition at several temperatures (red circles). The solid green curves show fitting results. The inset shows a schematic of the B transition in WSe_2, reflecting a transition between the VB2 valence and the CB1 conductance band. (c) Temperature dependence of the decay times determined from the PL decays (red circles) and transient differential reflectance (blue triangles) measurements. The solid curve shows the decay of bright trions based on Eq. (2). (d) Schematic of the intravalley relaxation of positive trions.

Figure 3. Temperature dependence of the valley relaxation time for a gate voltage of −40 V (red circles). The green filled curve is the valley relaxation time calculated from

Eq. (3). The inset presents a schematic of the relaxation process of the valley-polarized bright state of positive trions in WSe_2.

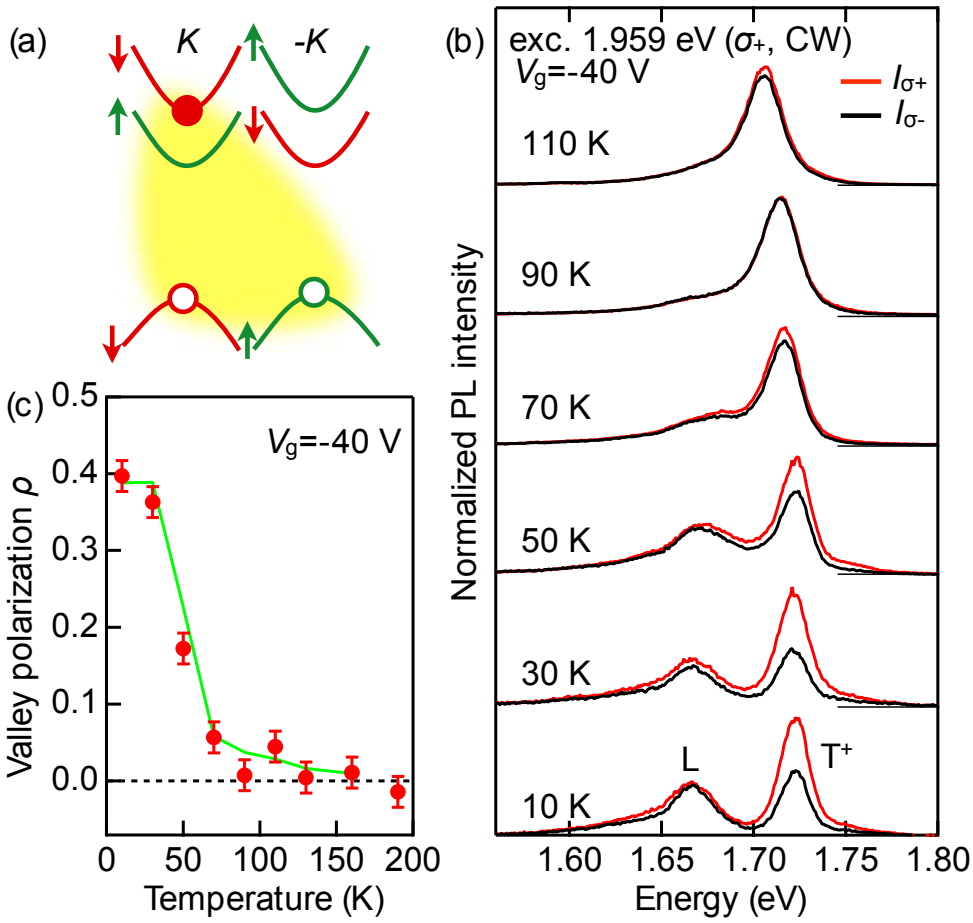

Figure 1 K. Shinokita *et al.*

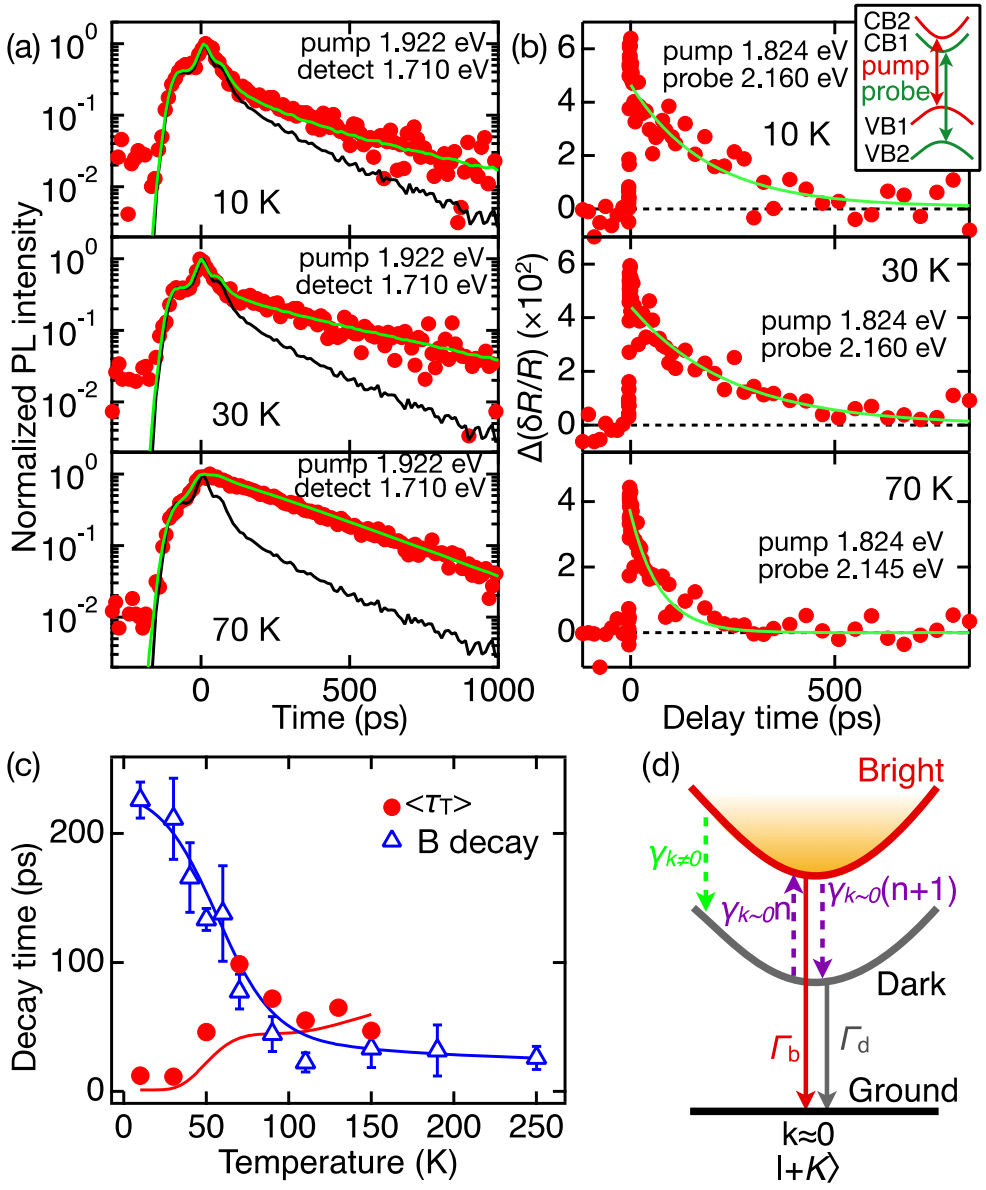

Figure 2 K. Shinokita *et al.*

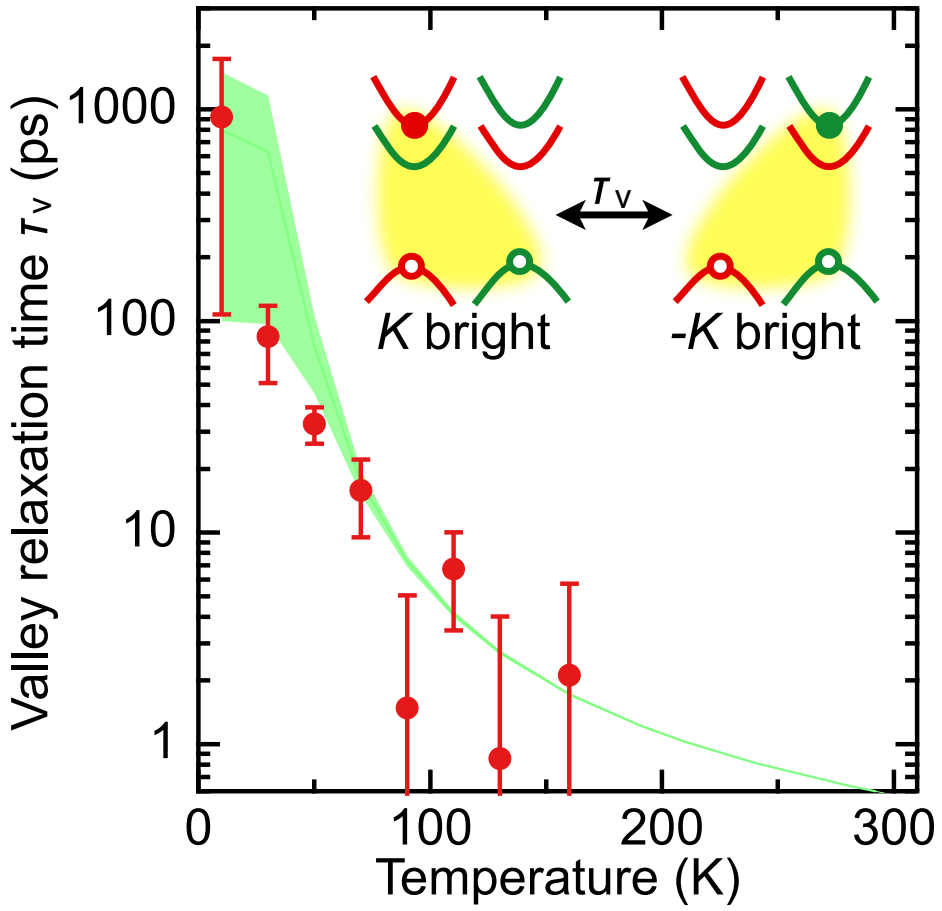

Figure 3 K. Shinokita *et al.*

References

[1] K. F. Mak, C. Lee, J. Hone, J. Shan, and T. F. Heinz, Phys. Rev. Lett. **105**, 136805 (2010).

[2] A. Splendiani, L. Sun, Y. Zhang, T. Li, J. Kim, C. Y. Chim, G. Galli, and F. Wang, Nano Lett. **10**, 1271 (2010).

[3] J. S. Ross, S. Wu, H. Yu, N. J. Ghimire, A. M. Jones, G. Aivazian, J. Yan, D. G. Mandrus, D. Xiao, W. Yao, and X. Xu, Nat. Commun. **4**, 1473 (2013).

[4] K. F. Mak, K. He, C. Lee, G. H. Lee, J. Hone, T. F. Heinz, and J. Shan, Nat. Mater. **12**, 207 (2013).

[5] A. Chernikov, T. C. Berkelbach, H. M. Hill, A. Rigosi, Y. Li, O. B. Aslan, D. R. Reichman, M. S. Hybertsen, and T. F. Heinz, Phys. Rev. Lett. **113**, 076802 (2014).

[6] K. He, N. Kumar, L. Zhao, Z. Wang, K. F. Mak, H. Zhao, and J. Shan, Phys. Rev. Lett. **113**, 026803 (2014).

[7] B. Zhu, X. Chen, and X. Cui, Sci. Rep. **5**, 9218 (2015).

[8] Y. Lin, X. Ling, L. Yu, S. Huang, A. L. Hsu, Y. H. Lee, J. Kong, M. S. Dresselhaus, and T. Palacios, Nano Lett. **14**, 5569 (2014).

[9] J. Yang, T. Lü, Y. W. Myint, J. Pei, D. Macdonald, J. C. Zheng, and Y. Lu, ACS Nano **9**, 6603 (2015).

[10] A. Boulesbaa, B. Huang, K. Wang, M. W. Lin, M. Mahjouri-Samani, C. Rouleau, K. Xiao, M. Yoon, B. Sumpter, A. Puretzky, and D. Geohegan, Phys. Rev. B **92**, 115443 (2015).

[11] S. Sim, J. Park, J. G. Song, C. In, Y. S. Lee, H. Kim, and H. Choi, Phys. Rev. B **88**, 075434 (2013).

[12] Y. Hoshi, T. Kuroda, M. Okada, R. Moriya, S. Masubuchi, K. Watanabe, T. Taniguchi, R. Kitaura, and T. Machida, Phys. Rev. B **95**, 241403(R) (2017).

[13] J. Pu and T. Takenobu, Adv. Mater. **30**, 1707627 (2018).

[14] G. Kioseoglou, A. T. Hanbicki, M. Currie, A. L. Friedman, D. Gunlycke, and B. T. Jonker, Appl. Phys. Lett. **101**, 221907 (2012).

[15] D. Xiao, G.-B. Liu, W. Feng, X. Xu, and W. Yao, Phys. Rev. Lett. **108**, 196802 (2012).

[16] K. F. Mak, K. He, J. Shan, and T. F. Heinz, Nat. Nanotechnol. **7**, 494 (2012).

[17] G. Wang, L. Bouet, D. Lagarde, M. Vidal, A. Balocchi, T. Amand, X. Marie, and B. Urbaszek, Phys. Rev. B **90**, 075413 (2014).

[18] A. T. Hanbicki, G. Kioseoglou, M. Currie, C. S. Hellberg, K. M. McCreary, A. L. Friedman, and B. T. Jonker, Sci. Rep. **6**, 18885 (2016).

[19] H. Zeng, J. Dai, W. Yao, D. Xiao, and X. Cui, Nat. Nanotechnol. **7**, 490 (2012).
[20] X. Xu, W. Yao, D. Xiao, and T. F. Heinz, Nat. Phys. **10**, 343 (2014).
[21] K. F. Mak, K. L. McGill, J. Park, and P. L. McEuen, Science **344**, 1489 (2014).
[22] R. Suzuki, M. Sakano, Y. J. Zhang, R. Akashi, D. Morikawa, A. Harasawa, K. Yaji, K. Kuroda, K. Miyamoto, T. Okuda, K. Ishizaka, R. Arita, and Y. Iwasa, Nat. Nanotechnol. **9**, 611 (2014).
[23] C. R. Zhu, K. Zhang, M. Glazov, B. Urbaszek, T. Amand, Z. W. Ji, B. L. Liu, and X. Marie, Phys. Rev. B **90**, 161302(R) (2014).
[24] S. Dal Conte, F. Bottegoni, E. A. A. Pogna, D. De Fazio, S. Ambrogio, I. Bargigia, C. D'Andrea, A. Lombardo, M. Bruna, F. Ciccacci, A. C. Ferrari, G. Cerullo, and M. Finazzi, Phys. Rev. B **92**, 235425 (2015).
[25] C. Mai, A. Barrette, Y. Yu, Y. G. Semenov, K. W. Kim, L. Cao, and K. Gundogdu, Nano Lett. **14**, 202 (2013).
[26] M. M. Glazov, T. Amand, X. Marie, D. Lagarde, L. Bouet, and B. Urbaszek, Phys. Rev. B **89**, 201302(R) (2014).
[27] S. Konabe, Appl. Phys. Lett. **109**, 073104 (2016).
[28] T. Yu and M. W. Wu, Phys. Rev. B **89**, 205303 (2014).
[29] K. Shinokita, X. Wang, Y. Miyauchi, K. Watanabe, T. Taniguchi, and K. Matsuda, Adv. Funct. Mater. 1900260 (2019).
[30] G. Plechinger, P. Nagler, A. Arora, A. Granados Del Águila, M. V Ballottin, T. Frank, P. Steinleitner, M. Gmitra, J. Fabian, P. C. M. Christianen, R. Bratschitsch, C. Schüller, and T. Korn, Nano Lett. **16**, 7899 (2016).
[31] Y. Miyauchi, S. Konabe, F. Wang, W. Zhang, A. Hwang, Y. Hasegawa, L. Zhou, S. Mouri, M. Toh, G. Eda, and K. Matsuda, Nat. Commun. **9**, 2598 (2018).
[32] A. M. Jones, H. Yu, N. J. Ghimire, S. Wu, G. Aivazian, J. S. Ross, B. Zhao, J. Yan, D. G. Mandrus, D. Xiao, W. Yao, and X. Xu, Nat. Nanotechnol. **8**, 634 (2013).
[33] M. Barbone, A. R.-P. Montblanch, D. M. Kara, C. Palacios-Berraquero, A. R. Cadore, D. De Fazio, B. Pingault, E. Mostaani, H. Li, B. Chen, K. Watanabe, T. Taniguchi, S. Tongay, G. Wang, A. C. Ferrari, and M. Atatüre, Nat. Commun. **9**, 3721 (2018).
[34] T. Yan, J. Ye, X. Qiao, P. Tan, and X. Zhang, Phys. Chem. Chem. Phys. **19**, 3176 (2017).
[35] T. Yan, X. Qiao, P. Tan, and X. Zhang, Sci. Rep. **5**, 15625 (2015).
[36] A. Singh, K. Tran, M. Kolarczik, J. Seifert, Y. Wang, K. Hao, D. Pleskot, N. M. Gabor, S. Helmrich, N. Owschimikow, U. Woggon, and X. Li, Phys. Rev. Lett.

117, 257402 (2016).

[37] G. Plechinger, P. Nagler, A. Arora, R. Schmidt, A. Chernikov, A. G. Del Águila, P. C. M. Christianen, R. Bratschitsch, C. Schüller, and T. Korn, Nat. Commun. **7**, 12715 (2016).

[38] F. Volmer, S. Pissinger, M. Ersfeld, S. Kuhlen, C. Stampfer, and B. Beschoten, Phys. Rev. B **95**, 235408 (2017).

[39] J. Huang, T. B. Hoang, T. Ming, J. Kong, and M. H. Mikkelsen, Phys. Rev. B **95**, 075428 (2017).

[40] E. J. Bushong, Yunqiu, Luo, K. M. McCreary, M. J. Newburger, S. Singh, B. T. Jonker, and R. K. Kawakami, 2D Mater. **5**, 011010 (2018).

[41] K. Shinokita, X. Wang, Y. Miyauchi, K. Watanabe, T. Taniguchi, S. Konabe, and K. Matsuda, Phys. Rev. B **99**, 245307 (2019).

[42] H. Zhong, Z. Zhang, H. Xu, C. Qiu, and L. M. Peng, AIP Adv. **5**, 057136 (2015).

[43] P. D. Cunningham, K. M. McCreary, and B. T. Jonker, J. Phys. Chem. Lett. **7**, 5242 (2016).

[44] A. Kormányos, G. Burkard, M. Gmitra, J. Fabian, V. Zólyomi, N. D. Drummond, and V. Fal'ko, 2D Mater. **2**, 022001 (2015).

[45] Y. You, X. X. Zhang, T. C. Berkelbach, M. S. Hybertsen, D. R. Reichman, and T. F. Heinz, Nat. Phys. **11**, 477 (2015).

[46] D. Lagarde, L. Bouet, X. Marie, C. R. Zhu, B. L. Liu, T. Amand, P. H. Tan, and B. Urbaszek, Phys. Rev. Lett. **112**, 047401 (2014).

[47] D. Y. Qiu, F. H. da Jornada, and S. G. Louie, Phys. Rev. Lett. **111**, 216805 (2013).

[48] Z. Wang, A. Molina-Sánchez, P. Altmann, D. Sangalli, D. De Fazio, G. Soavi, U. Sassi, F. Bottegoni, F. Ciccacci, M. Finazzi, L. Wirtz, A. C. Ferrari, A. Marini, G. Cerullo, and S. Dal Conte, Nano Lett. **18**, 6882 (2018).

[49] E. Liu, J. van Baren, Z. Lu, M. M. Altaiary, T. Taniguchi, K. Watanabe, D. Smirnov, and C. H. Lui, Phys. Rev. Lett. **123**, 027401 (2019).

[50] X. X. Zhang, Y. You, S. Y. F. Zhao, and T. F. Heinz, Phys. Rev. Lett. **115**, 257403 (2015).

[51] A. O. Slobodeniuk and D. M. Basko, 2D Mater. **3**, 035009 (2016).

[52] Z. Li, T. Wang, C. Jin, Z. Lu, Z. Lian, Y. Meng, M. Blei, S. Gao, T. Taniguchi, K. Watanabe, T. Ren, S. Tongay, L. Yang, D. Smirnov, T. Cao, and S.-F. Shi, Nat. Commun. **10**, 2469 (2019).

[53] E. Liu, J. Van Baren, Z. Lu, T. Taniguchi, and K. Watanabe, Arxiv **1906**, 02323 (2019).

[54] Y. Song and H. Dery, Phys. Rev. Lett. **111**, 026601 (2013).

[55] G. Wang, C. Robert, A. Suslu, B. Chen, S. Yang, S. Alamdari, I. C. Gerber, T. Amand, X. Marie, S. Tongay, and B. Urbaszek, Nat. Commun. **6**, 10110 (2015).

[56] C. Zhang, H. Wang, W. Chan, C. Manolatou, and F. Rana, Phys. Rev. B **89**, 205436 (2014).

[57] H. Yu, G. Bin Liu, P. Gong, X. Xu, and W. Yao, Nat. Commun. **5**, 3876 (2014).

[58] H. Yu, X. Cui, X. Xu, and W. Yao, Natl. Sci. Rev. **2**, 57 (2015).

[59] W. T. Hsu, Y. L. Chen, C. H. Chen, P. S. Liu, T. H. Hou, L. J. Li, and W. H. Chang, Nat. Commun. **6**, 8963 (2015).

[60] W. Zhao, Z. Ghorannevis, K. K. Amara, J. R. Pang, M. Toh, X. Zhang, C. Kloc, P. H. Tan, and G. Eda, Nanoscale **5**, 9677 (2013).

[61] N. Dong, Y. Li, Y. Feng, S. Zhang, X. Zhang, C. Chang, J. Fan, L. Zhang, and J. Wang, Sci. Rep. **5**, 14646 (2015).

[62] P. Tonndorf, R. Schmidt, P. Böttger, X. Zhang, J. Börner, A. Liebig, M. Albrecht, C. Kloc, O. Gordan, D. R. T. Zahn, S. Michaelis de Vasconcellos, and R. Bratschitsch, Opt. Express **21**, 4908 (2013).

[63] H. Sahin, S. Tongay, S. Horzum, W. Fan, J. Zhou, J. Li, J. Wu, and F. M. Peeters, Phys. Rev. B **87**, 165409 (2013).